Particle tracing around a static black hole in Weyl conformal gravity

Research Proposal · August 2020

DOI: 10.13140/RG.2.2.19703.85922

1 author:

Mohsen Fathi
USACH (Universidad de Santiago de Chile)
56 PUBLICATIONS **239** CITATIONS

Particle tracing around a static black hole in Weyl conformal gravity

Mohsen Fathi[1, *]

[1] *Instituto de Física y Astronomía, Universidad de Valparaíso, Avenida Gran Bretaña 1111, Valparaíso, Chile*

(Dated: August 23, 2020)

In this paper, we show that the recently calculated geodesics of massive and mass-less particles on a charged Weyl black hole, can be obtained directly by means of the Hamiltonian dynamics. The method applied here allows for three-dimensional simulations of the possible orbits and therefore, the spacetime curvature effects become more apparent. Significantly, and as a result of applying the method, it is observed that the particles show more tendency to fall onto the critical orbits.

keywords: Weyl gravity, charged static black holes, particle geodesics

PACS numbers: 04.50.+h,04.20.Jb,04.70.Bw

I. INTRODUCTION

Ever since the advent of general relativity, the notion of particle motion in curved spacetime has received a remarkable attention and has even entered classic pedagogical literature [1, 2]. This mainly stems in the success of the Riemannian description of exterior geometry of massive sources which helps the observer to introduce a set of geodesic equations to describe the motion of particles in the associated gravitational fields.

However, despite the successes of general relativity in being able to describe the propagation of gravitational waves [3–5] and black hole shadows [6], there are still some unexplained phenomena which have not been foreseen in general relativity and therefore, several scientists have been looking into alternative theories of gravity. The mentioned phenomena range from the flat galactic rotation curves [7] and the unexpected gravitational lensing [8], to the accelerated expansion of the universe [9–11] which have led to the emergence of dark matter/dark energy scenarios. The scientists' appeal to alternative theories is therefore along their endeavour to be able to explain the aforementioned phenomena with out being in need of the mentioned scenarios.

Accordingly, a conformally invariant theory of gravity, proposed by H. Weyl in 1918 [12], was revived by Riegert [13] and was then given a static spherically symmetric vacuum solution by Mannheim and Kazanas [14]. The solution has shown to be significant in being able to describe the flat galactic rotation curved as well as the late-time accelerated expansion of the universe [15–43].

In this paper, in particular, we deal with the geodesic motion of massive and mass-less particles in Weyl conformal gravity. Among other similar researches in the same field, recently, the motion of light rays and neutral particles around a particular charged static spherically symmetric black hole, introduced in Ref. [44], has been discussed in Refs. [45, 46]. In this work, same black hole and same particles are concerned, however, the difference from the similar works is the method which is employed in this paper. Unlike the usual treatment of the effective potential, here, we apply a canonical Hamiltonian dynamics to obtain the trajectories by solving simultaneously, the equations of motion. This way, the particles are indeed *traced* in their travel around the black hole.

The paper is organized as follows: in Sec. II, the Weyl field equations and the black hole solution are given concisely. In Sec. III, the method of Hamiltonian dynamics is introduced and the equations of motion are derived analytically, for both null (mass-less) and time-like (massive) particle trajectories. In Sec. IV, solving the equations of motion, all kind of possible trajectories are plotted and discussed. We summarize in Sec. V. Throughout the paper, the physical values are normalized by adopting $G = c = 1$.

II. THE BLACK HOLE SOLUTION

The common Einstein-Hilbert action is not applicable in Weyl theory of gravity, because the latter is given by the following action in terms of the Weyl conformal tensor $C_{\mu\nu\lambda\rho}$:

$$I_W = -\mathcal{K} \int \mathrm{d}^4x\sqrt{-g}\; C_{\mu\nu\rho\lambda}C^{\mu\nu\rho\lambda}, \tag{1}$$

* mohsen.fathi@postgrado.uv.cl

where $g = \det(g_{\mu\nu})$, $\mathcal{K}$ is a coupling constant, and

$$C_{\mu\nu\lambda\rho} = R_{\mu\nu\lambda\rho} - \frac{1}{2}\left(g_{\mu\lambda}R_{\nu\rho} - g_{\mu\rho}R_{\nu\lambda} - g_{\nu\lambda}R_{\mu\rho} + g_{\nu\rho}R_{\mu\lambda}\right) + \frac{R}{6}\left(g_{\mu\lambda}g_{\nu\rho} - g_{\mu\rho}g_{\nu\lambda}\right). \quad (2)$$

The action I_W is unchanged under the conformal transformation $g_{\mu\nu}(x) = e^{2\alpha(x)}g_{\mu\nu}(x)$, in which $2\alpha(x)$ is the local spacetime stretching. Combining Eqs. (1) and (2) and ignoring the Gauss-Bonnet total divergence, the action is reduced to [14, 47]

$$I_W = -2\mathcal{K}\int \mathrm{d}^4x\sqrt{-g}\,\left(R^{\alpha\beta}R_{\alpha\beta} - \frac{1}{3}R^2\right). \quad (3)$$

The principle of least action (i.e. $\frac{\delta I_W}{\delta g_{\alpha\beta}} = 0$), provides the Bach equation $W_{\alpha\beta} = 0$, with the Bach tensor defined as

$$W_{\alpha\beta} = \nabla^\sigma\nabla_\alpha R_{\beta\sigma} + \nabla^\sigma\nabla_\beta R_{\alpha\sigma} - \Box R_{\alpha\beta} - g_{\alpha\beta}\nabla_\sigma\nabla_\gamma R^{\sigma\gamma} - 2R_{\sigma\beta}R^\sigma{}_\alpha + \frac{1}{2}g_{\alpha\beta}R_{\sigma\gamma}R^{\sigma\gamma} - \frac{1}{3}\Big(2\nabla_\alpha\nabla_\beta R - 2g^{\alpha\beta}\Box R - 2RR_{\alpha\beta} + \frac{1}{2}g_{\alpha\beta}R^2\Big). \quad (4)$$

The spherically symmetric solution to the Bach equation, obtained by Mannheim and Kazanas, is of the form

$$\mathrm{d}s^2 = -B(r)\,\mathrm{d}t^2 + \frac{\mathrm{d}r^2}{B(r)} + r^2(\mathrm{d}\theta^2 + \sin^2\theta\,\mathrm{d}\phi^2) \quad (5)$$

in the usual Schwarzschild coordinates ($-\infty < t < \infty$, $r \geq 0$, $0 \leq \theta \leq \pi$ and $0 \leq \phi \leq 2\pi$), with the lapse function $B(r)$ defined as [14]

$$B(r) = 1 - \frac{\zeta(2 - 3\,\zeta\,\rho)}{r} - 3\,\zeta\,\rho + \rho\,r - \sigma\,r^2. \quad (6)$$

The coefficients ζ, ρ and σ are three-dimensional integration constants. The above solution reduces to the Schwarzschild-de Sitter solution for $\rho \to 0$ and therefore, at distances much smaller than $1/\rho$, it recovers general relativity. The Reissner–Nordström counterpart of this solution, corresponds to a charged massive source of charge q, characterized by the vector potential

$$A_\alpha = \left(\frac{q}{r}, 0, 0, 0\right), \quad (7)$$

for which, the Weyl field equations become

$$W_{\alpha\beta} = \frac{1}{4\mathcal{K}}\,T_{\alpha\beta}, \quad (8)$$

where $T_{\alpha\beta}$ is the energy-momentum tensor produced by $\boldsymbol{A}$ [48, 49]. In the same way and in Ref. [44], solving Eq. (8) for the source defined in Eq. (7), the following black hole solution was found in the weak field limit:

$$B(r) = 1 - \frac{r^2}{\lambda^2} - \frac{Q^2}{4r^2}, \quad (9)$$

in which

$$\frac{1}{\lambda^2} = \frac{3\,\tilde{m}}{\tilde{r}^3} + \frac{2\,c_1}{3}, \quad (10)$$

$$Q = \sqrt{2}\,\tilde{q}. \quad (11)$$

Here, $\tilde{m}$ and $\tilde{q}$ indicate the mass and the charge distribution of a spherically symmetric gravitating system of radius $\tilde{r}$. For $\lambda > Q$, this spacetime allows for two horizons; the event horizon r_+ and the cosmological horizon r_{++}, given by [46]

$$r_+ = \lambda\sin\left(\frac{1}{2}\arcsin\left(\frac{Q}{\lambda}\right)\right), \quad (12)$$

$$r_{++} = \lambda\cos\left(\frac{1}{2}\arcsin\left(\frac{Q}{\lambda}\right)\right). \quad (13)$$

The extremal black hole, characterized by the unique horizon $r_{\rm ex} = r_+ = r_{++} = \lambda/\sqrt{2}$ is obtained for $\lambda = Q$. For $\lambda < Q$ the system encounters a naked singularity. The causality is therefore confined to $r_+ < r < r_{++}$ and all the possible orbits happen in this region.

In the next section the basic canonical equations of motion are given in the context of Hamiltonian dynamics and the Hamilton-Jacobi formalism. This way, the relativistic geodesic equations are deduced trivially.

III. THE HAMILTONIAN DYNAMICS FOR PARTICLE MOTION

In classical dynamics, the Hamiltonian formalism gives the structure of the cotangent bundle associated with the base manifold, where the general solutions of the equations of motion are given. For a given Riemannian manifold $(\mathcal{M}, g_{\mu\nu})$, in the chart x^α, there is an associated cotangent bundle $T^*\mathcal{M}$ expressed by the coordinates (x^α, p_α), where p_α is the 4-momentum covector. For a solution curve $\gamma(\frac{\mathrm{d}x^\alpha}{\mathrm{d}\tau}, \frac{\mathrm{d}p_\alpha}{\mathrm{d}\tau})$[1] on $T^*\mathcal{M}$, the particles' trajectories on the base manifold are obtained by simply doing an identity transformation $\boldsymbol{i} : T^*\mathcal{M} \to \mathcal{M}$ which kills $\frac{\mathrm{d}p_\alpha}{\mathrm{d}\tau}$. Since (x^α, p_α) are indeed independent coordinates in the Hamiltonian formalism, the curve $\boldsymbol{\gamma}(\tau)$ can then be expressed as

$$\boldsymbol{\gamma} = \gamma\left(\frac{\partial\mathcal{H}}{\partial p_\alpha}, -\frac{\partial\mathcal{H}}{\partial x^\alpha}\right), \quad (14)$$

in which, the Hamiltonian $\mathcal{H}(x^\alpha, p_\alpha)$ constructs the particle dynamics and the 4-vector velocity $u^\alpha \equiv \frac{\mathrm{d}x^\alpha}{\mathrm{d}\tau}$ is defined relevantly. Moreover, since the motion happens in vacuum, we therefore can infer $p_\alpha = g_{\alpha\beta}u^\beta$, meaning that the 4-momentum is parallel to the tangential 4-velocity.

[1] The trajectory curves are supposed to be parametrized in terms of the proper time τ.

The motion is governed by the Hamilton-Jacobi equation [1]

$$\mathcal{H} = -\mu^2, \tag{15}$$

which together with the definition

$$\mathcal{H} = \frac{1}{2} g^{\alpha\beta} p_\alpha p_\beta = \frac{1}{2} g_{\alpha\beta} u^\alpha u^\beta, \tag{16}$$

provides the equation of the wave crests propagating on the cotangent bundle. The null and time-like trajectories are then specified by letting respectively $\mu^2 = 0$ and $\mu^2 = 1/2$. Applying the general metric (5) to the Eqs. (15) and (16), we get

$$-2\mu^2 = -\frac{E^2}{B(r)} + \frac{1}{B(r)}\left(\frac{\mathrm{d}r}{\mathrm{d}\tau}\right)^2 + r^2\left(\frac{\mathrm{d}\theta}{\mathrm{d}\tau}\right)^2 + \frac{L^2}{r^2\sin^2\theta}, \tag{17}$$

in which we have defined

$$E \doteq B(r)\left(\frac{\mathrm{d}t}{\mathrm{d}\tau}\right), \tag{18a}$$

$$L \doteq r^2\sin^2\theta\left(\frac{\mathrm{d}\phi}{\mathrm{d}\tau}\right), \tag{18b}$$

as the two constants of motion. Accordingly, the impact parameter of the trajectories can also be defined as

$$b \doteq \frac{L}{E}. \tag{19}$$

The impact parameter has an illuminating role in the identification of particle trajectories, as it measures the deviation of the world-lines from the straight line. Note that, the canonical Hamilton equations are based on the principle of the least action, which concerns about the shortest possible trajectories on which, the particles would travel. In Riemannian geometry, this principle leads to the geodesic equations, expressed as

$$\frac{\mathrm{d}u^\alpha}{\mathrm{d}\tau} + \Gamma^\alpha{}_{\beta\lambda} u^\beta u^\lambda = 0. \tag{20}$$

Accordingly, the spacetime metric (5), leads to the following set of geodesic equations:

$$\frac{\mathrm{d}^2 t}{\mathrm{d}\tau^2} + \frac{EB'(r)}{B(r)^2}\left(\frac{\mathrm{d}r}{\mathrm{d}\tau}\right) = 0, \tag{21}$$

$$\frac{\mathrm{d}^2 r}{\mathrm{d}\tau^2} - \frac{1}{2}\frac{B'(r)}{B(r)}\left(\frac{\mathrm{d}r}{\mathrm{d}\tau}\right)^2 - rB(r)\left(\frac{\mathrm{d}\theta}{\mathrm{d}\tau}\right)^2 - \frac{B(r)}{r^3\sin^2\theta}L^2 = 0, \tag{22}$$

$$\frac{\mathrm{d}^2\theta}{\mathrm{d}\tau^2} + \frac{2}{r}\left(\frac{\mathrm{d}r}{\mathrm{d}\tau}\right)\left(\frac{\mathrm{d}\theta}{\mathrm{d}\tau}\right) - \frac{\cot\theta}{r^4\sin^2\theta}L^2 = 0, \tag{23}$$

$$\frac{\mathrm{d}^2\phi}{\mathrm{d}\tau^2} + \frac{2L}{r^3\sin^2\theta}\left(\frac{\mathrm{d}r}{\mathrm{d}\tau}\right) + \frac{2L\cot\theta}{r^2\sin^2\theta}\left(\frac{\mathrm{d}\theta}{\mathrm{d}\tau}\right) = 0, \tag{24}$$

where prime stands for $\partial/\partial r$. The exact form of the trajectories is then given by solving, simultaneously, the Eqs. (17), (21),(22),(23) and (24). Indeed, the common way of determination of the trajectories, specially in the tracing of the null trajectories (ray-tracing), is to solve the canonical Hamilton equations. Here however, we solve numerically the aforementioned equations and plot the trajectories, respecting the types of motion. In the next section, the Hamilton-Jacobi equation is applied together with the geodesic equations for both the null and the time-like trajectories and the resultant forms of motion are demonstrated.

IV. PARTICLE TRACING

The Hamilton-Jacobi equation (15) is indeed the criterion, by which, the characteristic of the test particles are revealed. In this regard, for the light rays trajectories (i.e. null geodesics with $\mu = 0$), the Hamilton-Jacobi equation results in

$$\left(\frac{\mathrm{d}\theta}{\mathrm{d}\tau}\right)^2 = \frac{r^2\left(E^2 - (\frac{\mathrm{d}r}{\mathrm{d}\tau})^2\right) - L^2 B(r)\csc^2\theta}{r^4 B(r)}. \tag{25}$$

Interpolating Eq. (25) in the geodesic equations, results in a system of differential equations that characterize the motion of light rays in the black hole spacetime. To solve these equations numerically, the constants λ, Q, E and L have to be determined which the last two are given in the impact parameter b. The method of particle tracing we pursue, is based on obtaining the `InterpolatingFunction` for all the four spherical coordinates (t, r, θ, ϕ), by using the software *Mathematica*®. This way, the three-dimensional Cartesian coordinates (x, y, z) are then generated by applying

$$x(\tau) = r(\tau)\sin\theta(\tau)\cos\phi(\tau), \tag{26a}$$

$$y(\tau) = r(\tau)\sin\theta(\tau)\sin\phi(\tau), \tag{26b}$$

$$z(\tau) = r(\tau)\cos\theta(\tau), \tag{26c}$$

where

$$\phi(\tau) = \arctan\left(\frac{y(\tau)}{x(\tau)}\right), \tag{27a}$$

$$\theta(\tau) = \arctan\left(\frac{\sqrt{x(\tau)^2 + y(\tau)^2}}{z(\tau)}\right). \tag{27b}$$

The trajectories can then be plotted in the Cartesian space. In Fig. 1, several possible types of motion for the light rays have been plotted. The difference in the impact parameter, results in different fates for the infalling particles. As it is seen in the figure, the smallest impact parameters give rise to fall onto the event horizon. Increase

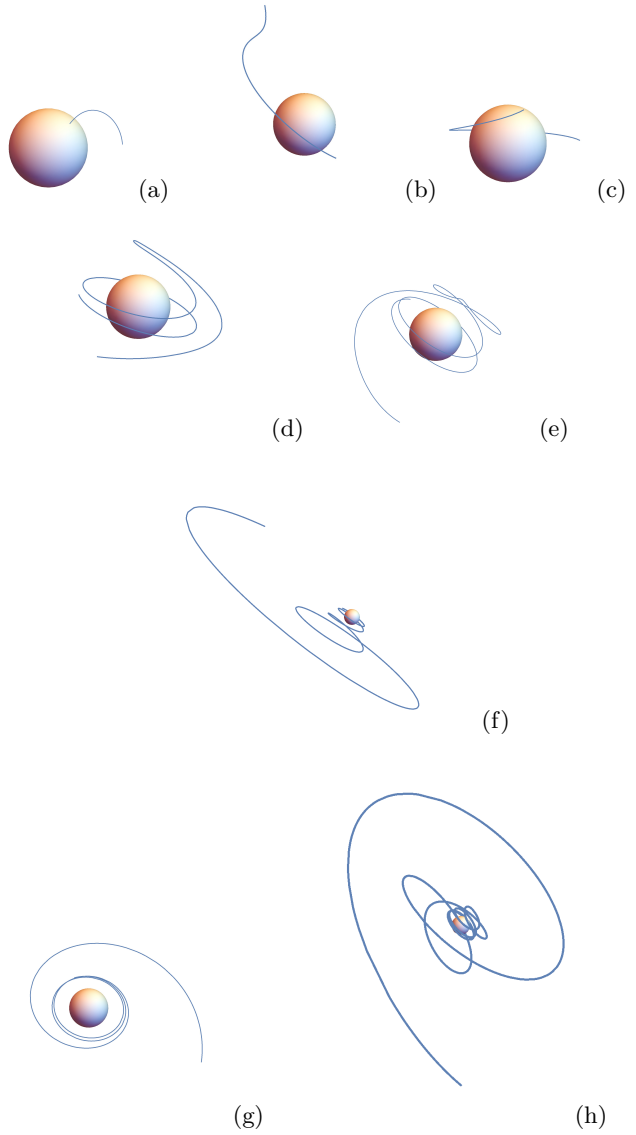

FIG. 1. The light ray trajectories on the black hole, considering $Q = 1$ and $\lambda = 2$ (in arbitrary length units) which correspond to $r_+ = 0.517638$ (the sphere in the plots). The trajectories have been plotted for (a) $b = \frac{2}{\sqrt{3}}$, (b) $b = 2.5$, (c) $b = 4$, (d-g) $b = 20$ and (h) $b = 40$.

in the impact parameter, changes the course of the trajectories to hyperbolic shapes which is the characteristic of deflection. Continuing the increase in b, the infalling particles will finally bounded in circular orbits around the black hole. In some cases, this is done through complicated orbits, according to the strong spacetime warping. However, the main objective in such orbits is to fall on an unstable circular orbit which defines the critical motion. So, the light ray trajectories on the black hole, are mostly of critical properties.

Now, switching to the motion of massive particles, the Hamilton-Jacobi equation (15) for $\mu^2 = 1/2$ provides

$$\left(\frac{\mathrm{d}\theta}{\mathrm{d}\tau}\right)^2 = \frac{-r^2\left(B(r) - E^2 + (\frac{\mathrm{d}r}{\mathrm{d}\tau})^2\right) - L^2 B(r)\csc^2\theta}{r^4 B(r)}, \tag{28}$$

which as before, is interpolated to the geodesic equations to construct the desired system of differential equations. The simultaneous solving of the equations, produces the trajectories, plotted in Fig. 2. The possible orbits range

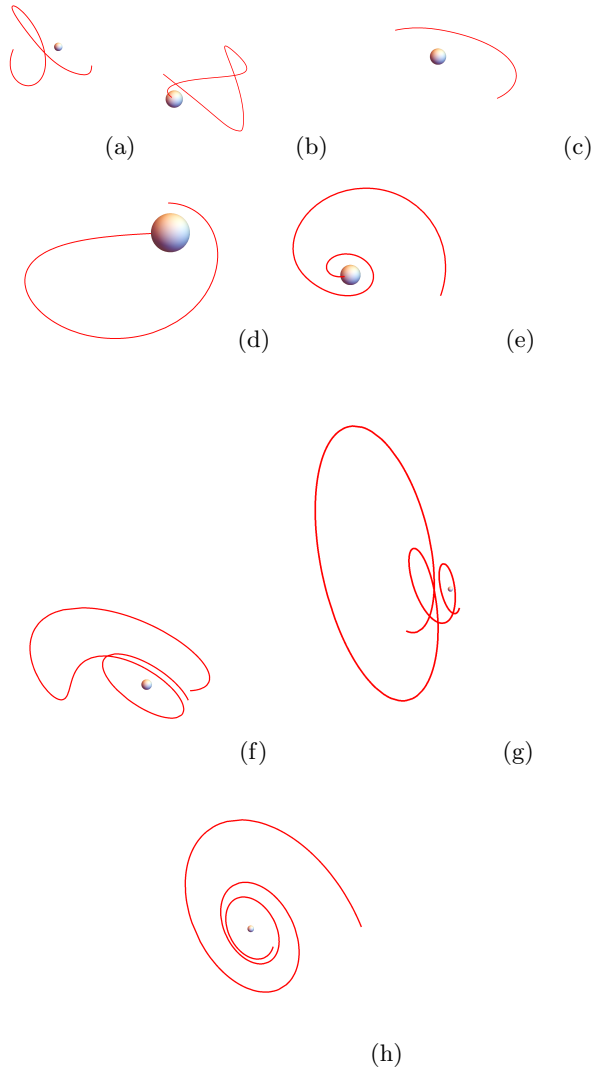

FIG. 2. The trajectories of massive test particles on the black hole, considering $Q = 1$ and $\lambda = 2$ (in arbitrary length units). The trajectories have been plotted for (a,b) $b = 1.3$, (c,d) $b = 2$, (e) $b = 4$ and (f-h) $b = 10$.

from hyperbolic trajectories to critical motions of both kinds. The fall onto the event horizon happens through both capturing and (spiralling) critical trajectories.

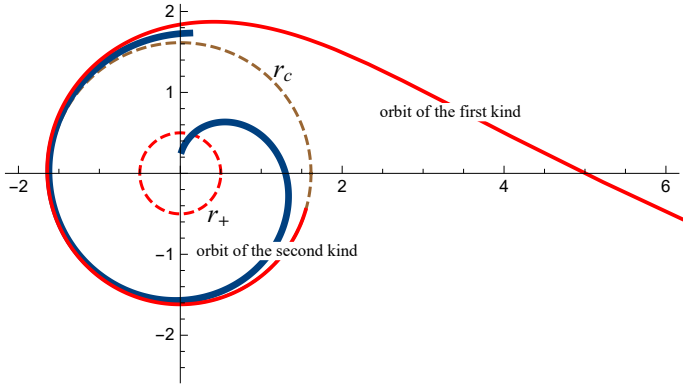

FIG. 3. The critical orbits of the first and the second kind. Here, r_c is the radius of the (un)stable circular orbits.

A. A note on the critical orbits

Among hundreds of possible orbits which are inferred from the geodesic equations, the critical type of motion is of great significance, because it can be related to the accreting particles in the black hole spacetime (time-like trajectories), as well as confining the black hole's shadow (null trajectories). These orbits are however ramified into distinguishable forms, resulting in different fates for the approaching particles (see for example Ref. [50]). According to Fig. 3, two types of critical orbits can be established by the particles: the orbit of the first kind, which allows the particle to be confined on a stable circular orbit around the black hole, and the orbit of the second kind which traps the trajectories onto the event horizon. Both of the orbits may follow after spiralling into the black hole region. For the light ray trajectories, in Fig. 1, items (d) to (h) are all critical trajectories of the first kind, whereas item (c) indicates that of the second kind. Since the trajectories of the first kind can travel to the distant observer, they are responsible to forming the photon rings and the black hole's shadow. For the particle trajectories plotted in Fig. 2, orbits of the first kind are those remarkably symmetric items (g) to (h). In particular, the item (h) demonstrates how an accretion disk can form around the black hole. Orbits of the second kind, given in items (d) and (e), clearly demonstrate spiralling onto the event horizon, which starts the in-fall from an unstable circular motion around the black hole.

V. DISCUSSION AND THE CONCLUDING REMARKS

The two-dimensional trajectory simulations given in Refs. [45, 46], would allow us comprehending the capabilities of the charged black hole in curving the spacetime around it. Such simulations however are confined to the equatorial plane and can only demonstrate the final fate of the approaching particles, regarding the possibility of being captured by the event horizon. The importance of the three-dimensional simulations is in their ability to indicate the variations in each type of orbit. For example, according to the simulations given in Figs. 1 and 2, in-fall onto a stable circular orbit can happen in completely different ways, including rather complicated shapes of spiralling. Same holds for deflecting trajectories which in two-dimensional simulations are given in terms of simple hyperbolic particle motions that travel inwardly or outwardly, depending on the point of approach and the particle's impact parameter. In the simulations given in this paper, same trajectories were shown to be of significant elevations from the equatorial plane, which highlights the rigorous spacetime warping caused by the black hole. The gravitational effects are therefore more apparent in the simulations given in this discussion.

In conclusion, we need to be aware of the strengths and weaknesses of each method of particle tracing. In general, the two-dimensional treatments allows for more feasible techniques in obtaining the exact analytical solutions to the equations of motion. They however lack demonstration of the true effects of spacetime curvature, caused by the black hole. Such features can be accentuated through three-dimensional treatments. This latter however results in much more complicated equations of motion, making the analytical calculation, a formidable task. This is were the numerical methods come to help. The particle tracing method employed in this paper, is one of the most popular techniques with a wide range of applications and here, in particular, has appeared rather useful in demonstrating the black hole capabilities in affecting its exterior geometry.

ACKNOWLEDGMENTS

I would like to express special thanks to my professors, M. Vučković and M. Zorotovic for supporting me during my progress in the course *Advanced Stellar Astrophysics*. I am in debt to my advisor, J.R. Villanueva, and also to M. Olivares, from whom I have learned a lot. This work has been supported by the Agencia Nacional de Investigación y Desarrollo (ANID) through DOCTORADO Grant No. 2019-21190382.

[1] C.W. Misner, K.S. Thorne, J.A. Wheeler, *Gravitation* (Princeton University Press, 2017). URL https://press.princeton.edu/books/hardcover/

9780691177793/gravitation
[2] R.M. Wald, *General Relativity* (Chicago Univ. Pr., Chicago, USA, 1984). URL https://doi.org/10.7208/chicago/9780226870373.001.0001
[3] B.P. Abbott, et al., Phys. Rev. Lett. **116**(6), 061102 (2016). URL https://doi.org/10.1103/PhysRevLett.116.061102
[4] B.P. Abbott, et al., Phys. Rev. Lett. **116**(24), 241103 (2016). URL https://doi.org/10.1103/PhysRevLett.116.241103
[5] B.P. Abbott, et al., Phys. Rev. Lett. **118**(22), 221101 (2017). URL https://doi.org/10.1103/PhysRevLett.118.221101. [Erratum: Phys. Rev. Lett.121,no.12,129901(2018)]
[6] K. Akiyama, et al., Astrophys. J. **875**(1), L1 (2019). URL http://doi.org/10.3847/2041-8213/ab0ec7
[7] V.C. Rubin, W.K. Ford, Jr., N. Thonnard, Astrophys. J **238**, 471 (1980). doi:10.1086/158003
[8] R. Massey, T. Kitching, J. Richard, Rept. Prog. Phys. **73**, 086901 (2010). URL https://doi.org/10.1088/0034-4885/73/8/086901
[9] A.G. Riess, et al., Astron. J. **116**, 1009 (1998). URL https://doi.org/10.1086/300499
[10] S. Perlmutter, et al., Astrophys. J. **517**, 565 (1999). URL https://doi.org/10.1086/307221
[11] P. Astier, arXiv e-prints arXiv:1211.2590 (2012)
[12] H. Weyl, Mathematische Zeitschrift **2**(3), 384 (1918). doi:10.1007/BF01199420. URL https://doi.org/10.1007/BF01199420
[13] R.J. Riegert, Phys. Rev. Lett. **53**, 315 (1984). doi:10.1103/PhysRevLett.53.315. URL https://link.aps.org/doi/10.1103/PhysRevLett.53.315
[14] P.D. Mannheim, D. Kazanas, Astrophysical Journal **342**, 635 (1989). URL https://doi.org/10.1086/167623
[15] P.D. Mannheim, Prog. Part. Nucl. Phys. **56**, 340 (2006). URL https://doi.org/10.1016/j.ppnp.2005.08.001
[16] R.K. Nesbet, Entropy **15**, 162 (2013). URL http://doi.org/10.3390/e15010162
[17] L. Knox, A. Kosowsky, arXiv:astro-ph/9311006 (1993). URL https://ui.adsabs.harvard.edu/abs/1993pncw.rept.....K
[18] A. Edery, M.B. Paranjape, Phys. Rev. **D58**, 024011 (1998). URL https://doi.org/10.1103/PhysRevD.58.024011
[19] D. Klemm, Class. Quant. Grav. **15**, 3195 (1998). URL https://doi.org/10.1088/0264-9381/15/10/020
[20] A. Edery, A.A. Methot, M.B. Paranjape, Gen. Rel. Grav. **33**, 2075 (2001). URL https://doi.org/10.1023/A:1013011312648
[21] S. Pireaux, Class. Quant. Grav. **21**, 1897 (2004). URL https://doi.org/10.1088/0264-9381/21/7/011
[22] S. Pireaux, Class. Quant. Grav. **21**, 4317 (2004). URL https://doi.org/10.1088/0264-9381/21/18/004
[23] A. Diaferio, L. Ostorero, Mon. Not. Roy. Astron. Soc. **393**, 215 (2009). URL https://doi.org/10.1111/j.1365-2966.2008.14205.x
[24] J. Sultana, D. Kazanas, Phys. Rev. **D81**, 127502 (2010). URL https://doi.org/10.1103/PhysRevD.81.127502
[25] A. Diaferio, L. Ostorero, V.F. Cardone, J. Cosmol. Astropart. Phys. **1110**, 008 (2011). URL https://doi.org/10.1088/1475-7516/2011/10/008
[26] P.D. Mannheim, Phys. Rev. **D85**, 124008 (2012). URL https://doi.org/10.1103/PhysRevD.85.124008
[27] M.R. Tanhayi, M. Fathi, M.V. Takook, Mod. Phys. Lett. **A26**, 2403 (2011). URL https://doi.org/10.1142/S0217732311036759
[28] J.L. Said, J. Sultana, K.Z. Adami, Phys. Rev. **D85**, 104054 (2012). URL https://doi.org/10.1103/PhysRevD.85.104054
[29] H. Lu, Y. Pang, C.N. Pope, J.F. Vazquez-Poritz, Phys. Rev. **D86**, 044011 (2012). URL https://doi.org/10.1103/PhysRevD.86.044011
[30] J.R. Villanueva, M. Olivares, J. Cosmol. Astropart. Phys. **1306**, 040 (2013). URL https://doi.org/10.1088/1475-7516/2013/06/040
[31] M. Mohseni, M. Fathi, Eur. Phys. J. Plus **131**, 21 (2016). URL https://doi.org/10.1140/epjp/i2016-16021-y
[32] K. Horne, Mon. Not. Roy. Astron. Soc. **458**(4), 4122 (2016). URL https://doi.org/10.1093/mnras/stw506
[33] Y.K. Lim, Q.h. Wang, Phys. Rev. **D95**(2), 024004 (2017). URL https://doi.org/10.1103/PhysRevD.95.024004
[34] G.U. Varieschi, General Relativity and Gravitation **42**(4), 929 (2010). doi:10.1007/s10714-009-0890-y. URL https://doi.org/10.1007/s10714-009-0890-y
[35] G. 't Hooft, arXiv e-prints arXiv:1011.0061 (2010). URL https://ui.adsabs.harvard.edu/abs/2010arXiv1011.0061T
[36] G. 't Hooft, arXiv e-prints arXiv:1009.0669 (2010). URL https://ui.adsabs.harvard.edu/abs/2010arXiv1009.0669T
[37] G. 't Hooft, Foundations of Physics **41**(12), 1829 (2011). doi:10.1007/s10701-011-9586-8. URL https://doi.org/10.1007/s10701-011-9586-8
[38] G.U. Varieschi, Z. Burstein, ISRN Astron. Astrophys. **2013**, 482734 (2013). URL https://doi.org/10.1155/2013/482734
[39] G.U. Varieschi, General Relativity and Gravitation **46**(6), 1741 (2014). doi:10.1007/s10714-014-1741-z. URL https://doi.org/10.1007/s10714-014-1741-z
[40] H.J. de Vega, N.G. Sanchez, arXiv e-prints arXiv:1304.0759 (2013)
[41] G.U. Varieschi, Galaxies **2**(4), 577 (2014). URL https://www.mdpi.com/2075-4434/2/4/577
[42] G.T. Hooft, arXiv e-prints arXiv:1410.6675 (2014)
[43] C. Deliduman, O. Kasikci, B. Yapiskan, arXiv e-prints arXiv:1511.07731 (2015)
[44] F. Payandeh, M. Fathi, Int. J. Theor. Phys. **51**, 2227 (2012). URL https://doi.org/10.1007/s10773-012-1102-1
[45] M. Fathi, M. Olivares, J.R. Villanueva, The European Physical Journal C **80**(1), 51 (2020). doi:10.1140/epjc/s10052-020-7623-5. URL https://doi.org/10.1140/epjc/s10052-020-7623-5
[46] M. Fathi, M. Kariminezhaddahka, M. Olivares, J. Villanueva, The European Physical Journal C **80**(5), 377 (2020). doi:10.1140/epjc/s10052-020-7945-3. URL https://doi.org/10.1140/epjc/s10052-020-7945-3
[47] D. Kazanas, P.D. Mannheim, Astrophysical Journal Supplement Series **76**, 431 (1991). doi:10.1086/191573. URL http://adsabs.harvard.edu/abs/1991ApJS...76..431K
[48] P.D. Mannheim, D. Kazanas, Phys. Rev. D **44**, 417 (1991). doi:10.1103/PhysRevD.44.417. URL https://link.aps.org/doi/10.1103/PhysRevD.44.417
[49] P.D. Mannheim, Annals of the New York Academy of Sciences **631**(1), 194 (1991). doi:10.1111/j.1749-6632.1991.tb52643.x. URL https:

//nyaspubs.onlinelibrary.wiley.com/doi/abs/10.1111/j.1749-6632.1991.tb52643.x

[50] S. Chandrasekhar, *The mathematical theory of black holes*. Oxford classic texts in the physical sciences (Oxford Univ. Press, Oxford, 2002). URL https://cds.cern.ch/record/579245